

It is possible that the decomposition of the complex in strong donor solvents arises from the weakening of the Ru(III)-cyanamide bond, although further study into the mechanism would have to confirm this.

From the above observations, it is clear that outer-sphere interactions with ligands can have a substantial effect on the degree of electronic interaction between donor and acceptor wave functions. Future studies will attempt to derive theoretical estimates of C_n and R as a function of solvent and the nature of the phenylcyanamide ligand. We have prepared the bridging

ligand 4-pyridylcyanamide anion and intend to prepare asymmetric ruthenium mixed-valence complexes. The Ru(III)-cyanamide chromophore is a probe of the extent of acceptor wave function interaction with the bridging ligand that will help evaluate the predicted¹³ solvent-dependent electronic coupling between donor and acceptor sites.

Acknowledgment. R.J.C. acknowledges the Natural Sciences and Engineering Research Council of Canada for their financial support and a University Research Fellowship.

Contribution from the Department of Chemistry,
Purdue University, West Lafayette, Indiana 47907

Non-Metal Redox Kinetics: Reactions of Trichloramine with Ammonia and with Dichloramine

Boudin S. Yiin and Dale W. Margerum*

Received October 30, 1989

Trichloramine reacts with excess NH_3 and base (B) with the rate expression $-\text{d}[\text{NCl}_3]/\text{d}t = 2k_{\text{B}}[\text{B}][\text{NH}_3][\text{NCl}_3]$, based on the overall stoichiometry $2\text{NCl}_3 + 3\text{NH}_3 + 3\text{OH}^- \rightarrow 3\text{NH}_2\text{Cl} + \text{N}_2 + 3\text{Cl}^- + 3\text{H}_2\text{O}$. The reaction is general-base assisted with k_{B} values ($\text{M}^{-2} \text{s}^{-1}$, 25.0 °C, $\mu = 0.50 \text{ M}$) of 4.46×10^3 for OH^- , 3.3×10^3 for PO_4^{3-} , and 22 for NH_3 . A water path with $k_{\text{H}_2\text{O}} = 2.2 \text{ M}^{-1} \text{s}^{-1}$ and an acidic phosphate path for H_2PO_4^- ($k_{\text{HB}} = 450 \text{ M}^{-2} \text{s}^{-1}$) are also found. The rate-determining step in the proposed mechanism is a Cl^+ transfer between NCl_3 and NH_3 to give HNCl_2 and NH_2Cl . This is followed by N_2 formation in a rapid base-assisted reaction between NCl_3 and HNCl_2 with the rate expression $-\text{d}[\text{NCl}_3]/\text{d}t = k_{\text{B}}'[\text{B}][\text{HNCl}_2][\text{NCl}_3]$, based on the stoichiometry $\text{NCl}_3 + \text{HNCl}_2 + 3\text{OH}^- \rightarrow \text{N}_2 + 2\text{HOCl} + 3\text{Cl}^- + \text{H}_2\text{O}$. Values of k_{B}' ($\text{M}^{-2} \text{s}^{-1}$, 25.0 °C, $\mu = 0.50 \text{ M}$) are 2.92×10^4 for HPO_4^{2-} and greater than 4×10^7 for OH^- . The HOCl released in the formation of N_2 reacts with excess NH_3 to give more NH_2Cl , which accounts for the overall stoichiometry of 1.5 NH_2Cl formed per NCl_3 . The reaction between NCl_3 and HNCl_2 is of critical importance in the explanation of breakpoint chlorination processes.

Introduction

Monochloramine, dichloramine, and trichloramine (nitrogen trichloride) are formed when excess chlorine is added to aqueous solutions that contain ammonia.¹⁻⁶ A process known as breakpoint chlorination occurs at Cl/N molar dose ratios greater than 1.6.⁵⁻⁷ Under these conditions, ammonia is oxidized to N_2 and the active chlorine species (HOCl , NH_2Cl , HNCl_2 , and NCl_3) are reduced to Cl^- . Chlorination provides the essential disinfection needed in the treatment of potable and waste water. The breakpoint process is vital in order to remove excess chloramines that are toxic to aquatic life. The mechanism of breakpoint chlorination has not been well understood, because many competing reactions can take place with the highly reactive chlorine species. In the past there has not been sufficient information about the kinetics of

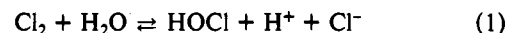
Table I. Ultraviolet Absorption Spectral Characteristics of Chlorine Species^a

species	λ , nm	ϵ , $\text{M}^{-1} \text{cm}^{-1}$
NCl_3	336 (max)	195 ^b
	360	130
HNCl_2	294 (max)	272 ^c
	360	≈ 3
NH_2Cl	243 (max)	461 ^c
	360	≈ 0
OCl^-	292 (max)	350 ^d
	360	≈ 5
HOCl	228 (max)	120 ^e
	360	≈ 0

^aThis work except where noted. ^bReferences 17 and 18. ^cReference 16. ^dReferences 14 and 15. ^eCalculated from ref 15.

individual reaction steps that lead to N_2 formation. We have addressed this problem by isolation of several of the reactions where NCl_3 is a reactant.

The addition of Cl_2 to water generates HOCl (eq 1), which reacts with NH_3 to form NH_2Cl (eq 2). Monochloramine is



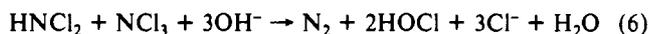
relatively stable in dilute solutions that contain excess ammonia. Hydrazine formation requires highly basic solutions and is a slow process.⁸ Dichloramine forms on the addition of more HOCl to monochloramine (eq 3) or by the disproportionation of monochloramine in acidic solutions (eq 4). Dichloramine is not stable

- (1) Weil, I.; Morris, J. C. *J. Am. Chem. Soc.* **1949**, *71*, 1664-1671.
- (2) Palin, A. T. *Waste Water Eng.* **1950**, *54*, 151-159, 189-200, 248-256.
- (3) Morris, J. C. In *Principles and Applications of Water Chemistry*; Faust, S. D., Hunter, J. V., Eds.; Wiley: New York, 1967; pp 23-53.
- (4) Gray, E. T., Jr.; Margerum, D. W.; Huffman, R. P. In *Organometals and Organometalloids, Occurrence and Fate in the Environment*; Brinkman, F. E., Bellama, J. M., Eds.; ACS Symposium Series 82; American Chemical Society: Washington, DC, 1978; pp 264-277.
- (5) Wei, I. W.; Morris, J. C. In *Dynamics of Breakpoint Chlorination*; Rubin, A. J., Ed.; Ann Arbor Science: Ann Arbor, MI, 1975; Chapter 13.
- (6) Margerum, D. W.; Gray, E. T.; Huffman, R. P. In *Organometals and Organometalloids, Occurrence and Fate in the Environment*; Brinkman, F. E., Bellama, J. M., Eds.; ACS Symposium Series 82; American Chemical Society: Washington, DC, 1978; pp 278-291.
- (7) Jolley, R. L.; Carpenter, J. H. In *Water Chlorination: Environmental Impact and Health Effects*; Jolley, R. L., Brungs, W. A., Cotruvo, J. A., Cumming, R. B., Mattice, J. S., Jacobs, V. A., Eds.; Ann Arbor Science: Ann Arbor, MI, 1983; Vol. 4, pp 1-47.

(8) Yagil, G.; Anbar, M. *J. Am. Chem. Soc.* **1962**, *84*, 1797-1803.



even in dilute solution, and its self-decomposition is frequently cited as a key step in breakpoint chlorination.⁵ Hand and Margerum⁹ showed that NH_3 inhibits the rate of decomposition of HNCl_2 , because it prevents the formation of NCl_3 . Their work proposed two critical reactions (eqs 5 and 6) in the decomposition



of dichloramine. The kinetics of the general-base- (B^-) assisted reaction between hypochlorous acid and dichloramine in eq 5 were determined.⁹ Indirect evidence showed that the rate of the reaction between HNCl_2 and NCl_3 in eq 6 is much faster than the reaction between two HNCl_2 molecules. Reactions 5 and 6 have been incorporated in some models of breakpoint chlorination.¹⁰

Although pure trichloramine is explosive, dilute NCl_3 in aqueous acid is relatively stable.^{11,12} The decomposition of NCl_3 in base was studied by Kumar, Shinness, and Margerum.¹³ In dilute base the reverse reaction in eq 5 predominates. This is a specific-base/general-acid-assisted reaction that gives HNCl_2 . Once again HNCl_2 and NCl_3 react rapidly in base (eq 6), and two NCl_3 molecules are consumed each time one NCl_3 reacts with base.

Although NH_3 helps to stabilize solutions of NH_2Cl and HNCl_2 , it has the opposite effect with NCl_3 . The present work examines the effect of NH_3 on the rate of decomposition of NCl_3 in the presence of OH^- or buffers. We propose a Cl^+ -transfer reaction between NCl_3 and NH_3 to give HNCl_2 and NH_2Cl as the initial products. The formation of HNCl_2 in the presence of NCl_3 leads to the decomposition reaction in eq 6. This gives a stoichiometry with two NCl_3 molecules consumed for each one that reacts with NH_3 . We also examine the kinetics of the direct reaction between HNCl_2 and NCl_3 and show that N-N bond formation is a fast, base-assisted process. We propose that this is a key reaction in breakpoint chlorination.

Experimental Section

Reagents. A 5% solution of sodium hypochlorite (Mallinckrodt) was used as the source of active chlorine. The concentration of stock OCl^- solutions was determined spectrophotometrically at 292 nm (Table I, $\epsilon = 350 \text{ M}^{-1} \text{ cm}^{-1}$).^{14,15} The NH_3 stock solution was standardized with HClO_4 , with bromocresol green as the indicator. Phosphate buffer was prepared from Na_2HPO_4 and NaH_2PO_4 . Ionic strength was maintained at 0.50 M with recrystallized sodium perchlorate.

Preparation of Chloramines. Monochloramine solutions were prepared by mixing OCl^- and NH_3 solutions through a T-mixer at pH 9–10, and NH_3 was in slight excess in the final solution. Dilute dichloramine solutions ($\approx 1 \text{ mM}$) were prepared by dropwise addition of 0.1 M perchloric acid to the NH_2Cl solutions until the final pH was 3.5–4.0. The reaction mixture was allowed to stand at least 4 h to complete the formation of HNCl_2 . The solutions were placed in a stoppered flask with no headspace to avoid volatilization of HNCl_2 . Solutions prepared in this way were stable for 1 day. It is important to keep the pH above 3 during the preparation, because if any NCl_3 forms it reacts with HNCl_2 . The HNCl_2 solutions were standardized spectrophotometrically at 294 nm (Table I, $\epsilon = 272 \text{ M}^{-1} \text{ cm}^{-1}$).¹⁶ Trichloramine solutions were prepared from 3:1 mixtures of HOCl and NH_3 with both solutions initially at pH 3–4. The NH_3 and HOCl solutions were mixed through a T-mixer, and the resulting NCl_3 solutions were kept overnight in the dark to allow all

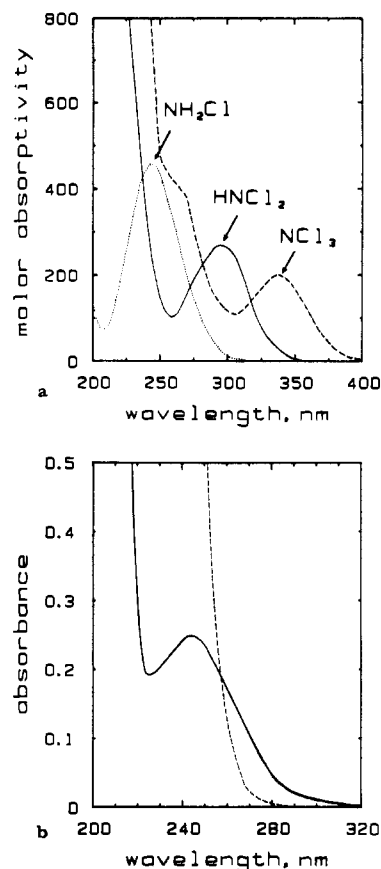


Figure 1. (a) Spectral characteristics of chloramine species: (---) NH_2Cl , (—) HNCl_2 , and (---) NCl_3 . (b) Spectra of SO_3^{2-} and of the product of the NH_3 and NCl_3 reaction: (---) sulfite ($[\text{SO}_3^{2-}] = 2.21 \times 10^{-2} \text{ M}$, $[\text{NaOH}] = 0.050 \text{ M}$); (—) product ($[\text{NH}_3] = 5.00 \times 10^{-3} \text{ M}$, $[\text{NCl}_3]_i = 3.85 \times 10^{-4} \text{ M}$, $[\text{NaOH}] = 0.050 \text{ M}$).

side reactions to go to completion. The NCl_3 solutions were standardized spectrophotometrically at 336 nm (Table I, $\epsilon = 195 \text{ M}^{-1} \text{ cm}^{-1}$).^{17,18} The amount of NCl_3 formed was always less than the initial NH_3 concentration due to the formation of N_2 .⁹ The acidic NCl_3 solution is relatively stable; however, the vapor pressure of NCl_3 is 150 mmHg at room temperature,¹⁹ so the NCl_3 solutions were also stored in stoppered flasks with no headspace.

Methods. Spectrophotometric measurements were made with a Perkin-Elmer 320 spectrophotometer interfaced to a PE 3600 data station. An Orion Model 601A Research digital pH meter equipped with a Corning combination electrode was used for pH measurements. The pH values were corrected to $\text{p}[\text{H}^+]$ values at 25.0 °C and $\mu = 0.50 \text{ M}$ based on electrode calibration by titration of standard HClO_4 with a standard NaOH solution. The kinetics were measured with either a Durrum or a Hi-Tech stopped-flow spectrophotometer interfaced to a Zenith 151 PC with a MetraByte DASH-16 A/D interface card. All solutions were thermostated at 25.0 ± 0.1 °C. The reaction of excess NH_3 with NCl_3 was monitored by the disappearance of NCl_3 at 360 nm (side of the absorption peak) in order to avoid interference from HNCl_2 and OCl^- (Table I and Figure 1a). The rate expression for the loss of NCl_3 is given in eq 7. A factor of 2 is introduced in this equation because NH_3 and

$$-d[\text{NCl}_3]/dt = 2k_{\text{obsd}}[\text{NCl}_3] \quad (7)$$

NCl_3 react with 1:2 stoichiometry. Pseudo-first-order rate constants (k_{obsd}) were analyzed over at least four half-lives on the basis of least-squares nonlinear regression of $\log(A_\infty - A_t)$ vs time, where A_∞ represents the final absorbance and A_t is the absorbance at any time. The k_{obsd} values were corrected for the mixing effect for both stopped-flow instruments.²⁰

The fast reaction of HNCl_2 with NCl_3 was studied under second-order unequal concentration conditions with HNCl_2 in slight excess. The

(9) Hand, V. C.; Margerum, D. W. *Inorg. Chem.* **1983**, *22*, 1449–1456.

(10) Jafvert, C. T. Ph.D. Thesis, The University of Iowa, Iowa City, IA, 1985.

(11) Mellor, J. W. *A Comprehensive Treatise in Inorganic and Theoretical Chemistry*; Longmans Green: New York, 1928; p 598.

(12) Koviach, P.; Lowery, M. K.; Field, K. W. *Chem. Rev.* **1970**, *70*, 639–665.

(13) Kumar, K.; Shinness, R. W.; Margerum, D. W. *Inorg. Chem.* **1987**, *26*, 3430–3434.

(14) Soulard, M.; Block, F.; Hatterer, A. *J. Chem. Soc., Dalton Trans.* **1981**, 2300–2310.

(15) Gray, E. T. Ph.D. Thesis, Purdue University, West Lafayette, IN 1977.

(16) Kumar, K.; Day, R. A.; Margerum, D. W. *Inorg. Chem.* **1986**, *25*, 4344–4350.

(17) Hand, V. C. Ph.D. Thesis, Purdue University, West Lafayette, IN 1982.

(18) Walker, D. M. M.S. Thesis, Purdue University, West Lafayette, IN 1981.

(19) *The Merck Index*, 9th ed.; Windholz, M., Ed.; Merck: Rahway, NJ, 1976; p 858.

(20) Dickson, P. N.; Margerum, D. W. *Anal. Chem.* **1986**, *58*, 3153–3158.

Table II. Yield of NH₂Cl in the Reaction between NH₃ and NCl₃^a

pH	[NH ₂ Cl] _f /[NCl ₃] _i
13.0	1.35
12.7	1.43
12.7	1.68
12.7	1.78
10.3	1.66
8.5	1.67
7.1	1.23
1.5 ± 0.2 av	

^aConditions: [NH₃]_T = (5.0–15.0) × 10⁻³ M, [NCl₃]_i is the initial concentration of NCl₃ and equals (1.79–3.85) × 10⁻⁴ M. [NH₂Cl]_f is the final concentration of NH₂Cl and is determined spectrophotometrically at 243 nm, ε = 461 M⁻¹ cm⁻¹.

disappearance of NCl₃ was again monitored at 360 nm. The second-order rate constants for the HNCl₂ and NCl₃ reaction in p[H⁺] 6–7 phosphate buffer were calculated on the basis of the second-order rate law for unequal concentrations (eq 8),²¹ where [A]₀ and [B]₀ (in excess)

$$\ln \left(1 + \frac{\Delta_0}{[A]_0} \frac{A_0 - A_\infty}{A_t - A_\infty} \right) = \ln \left(\frac{[B]_0}{[A]_0} \right) + \Delta_0 k_{2nd} t \quad (8)$$

are the initial concentrations of NCl₃ and HNCl₂, respectively; Δ₀ = [B]₀ - [A]₀, and k_{2nd} is the second-order rate constant (M⁻¹ s⁻¹). Individual HNCl₂ and NCl₃ solutions decompose with moderate speed in base.^{9,13} In order to study the reactions in basic media, a sequential-mixing mode was used with the Hi-Tech stopped-flow instrument. Three syringes were used that contained solutions of NCl₃, HNCl₂, and NaOH, respectively. The NCl₃ and NaOH solutions mixed first, and within 2 ms, this mixture was pushed into the stopped-flow mixing chamber (1.60-cm cell path)²² where it encountered the HNCl₂ solution. Therefore, neither HNCl₂ nor NCl₃ was prepared in base.

Both k_{obsd} and k_{2nd} values were averaged over at least three trials for each set of conditions.

Results

Stoichiometry of NH₂Cl Formation. Figure 1b shows the UV absorbance of the reaction products when NCl₃ (0.385 mM) is mixed with excess NH₃ (5.00 mM) in 0.050 M NaOH. The absorbance between 320 and 220 nm is identical with the NH₂Cl spectrum (Figure 1a), but below 220 nm there is an absorbance increase that is not due to NH₂Cl. Although NCl₃ and HNCl₂ have molar absorptivities as large as 81 000 and 21 000 M⁻¹ cm⁻¹, respectively, in the wavelength region from 200–220 nm, the lack of absorbance at 336 and 294 nm (Table I and Figure 1b) indicates that negligible amounts of these species remain in solution. The rate constants for the loss of NCl₃ and HNCl₂ also indicate that they should not be present in appreciable concentrations after 20 min when the spectrum was measured. Valentine et al.^{23,24} reported a similar spectrum when 9 mM NH₂Cl was allowed to decompose for 208 h at pH 8.0. They attributed the spectrum to some remaining NH₂Cl and to an "unidentified decomposition product". We performed several tests to verify that our principal product is NH₂Cl. The kinetics of its reaction with excess SO₃²⁻ (4.43 × 10⁻² M) in 0.050 M NaOH (μ = 0.50 M, 25.0 °C) were measured at 270 nm by stopped-flow methods. Figure 1b shows the absorbance of SO₃²⁻ at this concentration and shows why 270 nm was selected to follow the reaction. The k_{obsd} value was 0.175 ± 0.003 s⁻¹, which agrees with the rate constant of 0.17 s⁻¹ calculated from the direct study of SO₃²⁻ and NH₂Cl under these conditions.²⁵ The absorbance change (A₀ - A_∞) at 270 nm corresponds to the value expected from calculation of the NH₂Cl concentration at its λ_{max} (243 nm). This indicates that at least 95% of the absorbing product is NH₂Cl. In another test, NaI was added to the product and I₃⁻ formed at neutral pH. Valentine

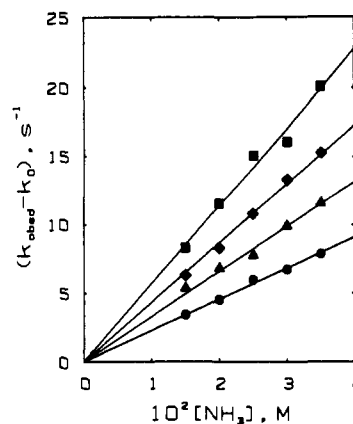


Figure 2. NH₃ dependence of the reaction between NH₃ and NCl₃ at different OH⁻ concentrations: (●) [OH⁻] = 0.050 M; (▲) [OH⁻] = 0.075 M; (◆) [OH⁻] = 0.100 M; (■) [OH⁻] = 0.125 M. Slope = k_{OH}[OH⁻] + k_{H₂O}.

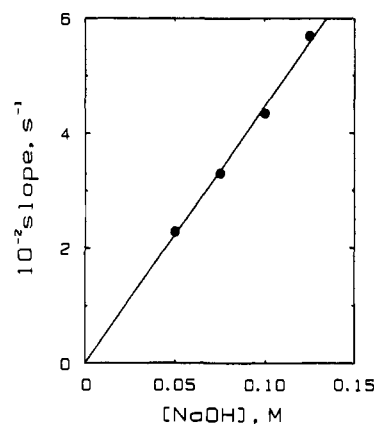
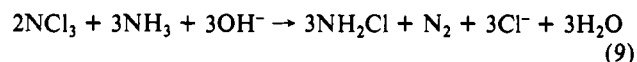


Figure 3. [OH⁻] dependence of the reaction between NH₃ and NCl₃. Slope: k_{OH} = 4.46 (±0.06) × 10³ M⁻² s⁻¹.

et al.^{23,24} reported that their unidentified product did not oxidize I⁻. We conclude that under our conditions the products that absorb below 220 nm are minor components (<5% of the initial NCl₃) that may have large molar absorptivities at low wavelengths but do not contribute to the absorbance above 240 nm.

Table II gives the yield of NH₂Cl measured spectrophotometrically at 243 nm after the decomposition of NCl₃ occurs in excess NH₃ at different p[H⁺] values. (The volatility of NCl₃ is the major source of error in these experiments.) The results show that the yield is 1.5 ± 0.2 NH₂Cl molecules per initial NCl₃. This corresponds to the stoichiometry in eq 9.



NCl₃ and NH₃ Kinetics in NaOH. The reaction between NCl₃ and NH₃ was studied in 0.050–0.125 M NaOH solutions under pseudo-first-order conditions with [NH₃] = 0.015–0.035 M and NCl₃ as the limiting reagent. Excellent first-order absorbance decays were observed. The reaction conditions and kinetic data are listed in Table III. In this pH range, NCl₃ decomposes by reactions with OH⁻ as well as with NH₃. The contribution from the NCl₃ base decomposition (k₀) has both a first-order and a second-order dependence in hydroxide ion concentration as expressed in eq 10,¹³ where k₀' = 1.6 × 10⁻⁶ s⁻¹, k₁' = 8 M⁻¹ s⁻¹,

$$k_0 = k_0' + k_1'[\text{OH}^-] + k_2'[\text{OH}^-]^2 \quad (10)$$

and k₂' = 890 M⁻² s⁻¹. The calculated k₀ values for the NCl₃ base decomposition are 25–64% of the k_{obsd} values. The (k_{obsd} - k₀) values depend on both NH₃ and OH⁻ concentrations (eq 11). In

$$k_{\text{obsd}} - k_0 = (k_{\text{OH}}[\text{OH}^-] + k_{\text{H}_2\text{O}})[\text{NH}_3] \quad (11)$$

Figure 2, the (k_{obsd} - k₀) values are plotted against [NH₃] for four

- (21) Espenson, J. H. *Chemical Kinetics and Reaction Mechanisms*; McGraw-Hill: New York, 1981; pp 16–24.
 (22) Wang, Y. L. Ph.D. Thesis, Purdue University, West Lafayette, IN 1989.
 (23) Jafvert, C. T.; Valentine, R. L. *Water Res.* **1987**, *21*, 967–973.
 (24) Valentine, R. L.; Brandt, K. I.; Jafvert C. T. *Water Res.* **1986**, *20*, 1067–1074.
 (25) Yiin, B. S.; Walker, D. M.; Margerum, D. W. *Inorg. Chem.* **1987**, *26*, 3435–3441.

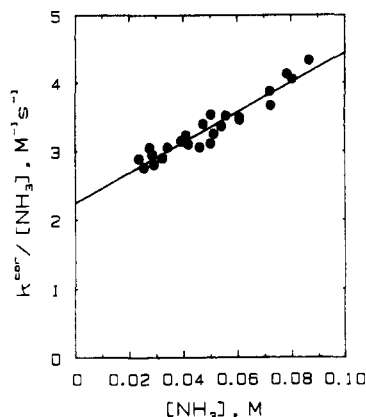


Figure 4. $[\text{NH}_3]^2$ dependence of the reaction between NH_3 and NCl_3 . The slope corresponds to $k_{\text{NH}_3} = 22 (\pm 1) \text{ M}^{-2} \text{ s}^{-1}$ and the intercept corresponds to $k_{\text{H}_2\text{O}} = 2.2 (\pm 0.1) \text{ M}^{-1} \text{ s}^{-1}$.

different sets of OH^- concentrations (0.050, 0.075, 0.100, and 0.125 M). The intercept of each linear relationship equals zero within statistical error. The values of the slopes in Figure 2 correspond to $k_{\text{OH}}[\text{OH}^-] + k_{\text{H}_2\text{O}}$. Figure 3 shows that the slopes are directly proportional to $[\text{OH}^-]$ and gives a k_{OH} value of $4.46 (\pm 0.06) \times 10^3 \text{ M}^{-2} \text{ s}^{-1}$. The zero intercept in Figure 3 indicates that the $k_{\text{H}_2\text{O}}$ value (the contribution from the water-assisted path of the NH_3 and NCl_3 reaction) is very small and cannot be determined under these conditions.

NCl_3 and NH_3 Kinetics Buffered by $\text{NH}_4^+/\text{NH}_3$. The k_{obsd} values and experimental conditions for the reaction between a large excess NH_3 and NCl_3 without additional buffer are given in Table III. The $\text{p}[\text{H}^+]$ values are in the range of 8.92–10.13 and the total ammonia concentration ($[\text{NH}_3]_{\text{T}} = [\text{NH}_3] + [\text{NH}_4^+]$) varies from 0.060 to 0.100 M. The $\text{p}K_{\text{a}}$ for NH_4^+ is 9.32 at $\mu = 0.50 \text{ M}$, 25.0 °C.²⁶ Correction for the k_0 term in eq 10 is negligible in this $\text{p}[\text{H}^+]$ range. The $k_{\text{OH}}[\text{OH}^-][\text{NH}_3]$ term is subtracted from k_{obsd} values to give k^{cor} values that have first-order and second-order dependences on the NH_3 concentration (eq 12). Equation 13

$$k^{\text{cor}} = k_{\text{NH}_3}[\text{NH}_3]^2 + k_{\text{H}_2\text{O}}[\text{NH}_3] \quad (12)$$

$$k^{\text{cor}}/[\text{NH}_3] = k_{\text{NH}_3}[\text{NH}_3] + k_{\text{H}_2\text{O}} \quad (13)$$

is obtained by rearrangement of eq 12. A least-squares regression plot of $k^{\text{cor}}/[\text{NH}_3]$ vs $[\text{NH}_3]$ gives a slope, $k_{\text{NH}_3} = 22 (\pm 1) \text{ M}^{-2} \text{ s}^{-1}$, and an intercept, $k_{\text{H}_2\text{O}} = 2.2 (\pm 0.1) \text{ M}^{-1} \text{ s}^{-1}$ (Figure 4).

NCl_3 and NH_3 Kinetics Buffered by $\text{HPO}_4^{2-}/\text{PO}_4^{3-}$. The kinetic data obtained in $\text{HPO}_4^{2-}/\text{PO}_4^{3-}$ buffered solutions ($[\text{PO}_4^{3-}]_{\text{T}} = 0.030\text{--}0.070 \text{ M}$, $\text{p}K_{\text{a}} = 11.34$ for HPO_4^{2-} at $\mu = 0.50 \text{ M}$, 25.0 °C²⁷) at a constant $\text{p}[\text{H}^+]$ value of 11.06 are listed in Table III. In another series of experiments, $[\text{PO}_4^{3-}]_{\text{T}}$ was kept constant at 0.050 M and the $\text{p}[\text{H}^+]$ values were varied from 10.54 to 11.91. The previously determined k_0 , k_{OH} , and k_{NH_3} values are used to simplify the calculation of the rate constants for the PO_4^{3-} -assisted reaction path. The k^{cor} values are calculated by subtraction of the $(k_0 + k_{\text{OH}}[\text{OH}^-][\text{NH}_3] + k_{\text{NH}_3}[\text{NH}_3]^2)$ term from the k_{obsd} values. Equation 14 gives the k^{cor} dependence on $[\text{PO}_4^{3-}]$ and

$$k^{\text{cor}} = (k_{\text{PO}_4}[\text{PO}_4^{3-}] + k_{\text{H}_2\text{O}})[\text{NH}_3] \quad (14)$$

$[\text{NH}_3]$. A plot of $k^{\text{cor}}/[\text{NH}_3]$ vs $[\text{PO}_4^{3-}]$ for both sets of data is given in Figure 5. The slope gives $k_{\text{PO}_4} = 3.3 (\pm 0.4) \times 10^3 \text{ M}^{-2} \text{ s}^{-1}$, and the intercept gives $k_{\text{H}_2\text{O}} = 21 (\pm 12) \text{ M}^{-1} \text{ s}^{-1}$. A relatively large uncertainty is expected for the $\text{p}[\text{H}^+]$ measurements at high pH , which may account for some of the scattering seen in Figure 5.

NCl_3 and NH_3 Kinetics Buffered by $\text{H}_2\text{PO}_4^-/\text{HPO}_4^{2-}$. The kinetic data obtained in $\text{H}_2\text{PO}_4^-/\text{HPO}_4^{2-}$ buffer solution ($[\text{HPO}_4^{2-}]_{\text{T}} = 0.050 \text{ M}$, $\text{p}K_{\text{a}} = 6.46$ for H_2PO_4^- at $\mu = 0.50 \text{ M}$,

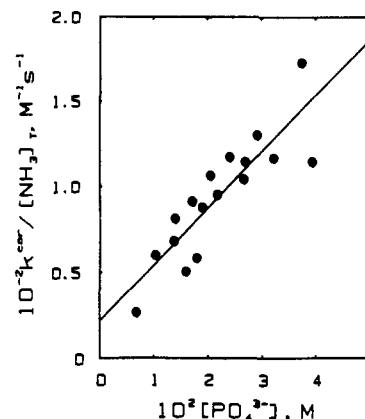


Figure 5. PO_4^{3-} dependence of the reaction between NH_3 and NCl_3 .

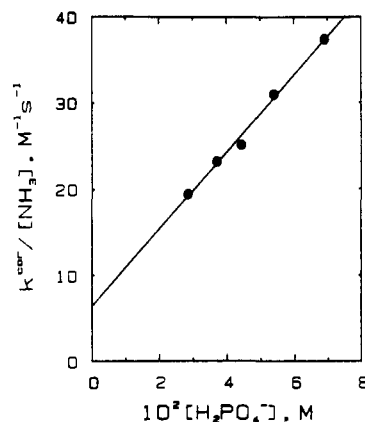


Figure 6. H_2PO_4^- dependence of the pseudo-first-order rate constant for the reaction between NH_3 and NCl_3 at $\text{p}[\text{H}^+]$ 6.10–6.85.

25.0 °C²⁸) in the $\text{p}[\text{H}^+]$ range 6.10–6.85 are given in Table III. In this buffer system the $(k_0 + k_{\text{OH}}[\text{OH}^-][\text{NH}_3] + k_{\text{NH}_3}[\text{NH}_3]^2)$ term is negligible and the k_{obsd} values depend on the H_2PO_4^- concentration (eq 15) rather than the HPO_4^{2-} concentration. The

$$k_{\text{obsd}} = (k_{\text{H}_2\text{PO}_4}[\text{H}_2\text{PO}_4^-] + k_{\text{H}_2\text{O}})[\text{NH}_3] \quad (15)$$

$k_{\text{obsd}}/[\text{NH}_3]$ values increase with increasing $[\text{H}_2\text{PO}_4^-]$ as shown in Figure 6. The slope of the least-squares line gives $k_{\text{H}_2\text{PO}_4} = 450 (\pm 20) \text{ M}^{-2} \text{ s}^{-1}$ and the intercept yields $k_{\text{H}_2\text{O}} = 6 (\pm 1) \text{ M}^{-1} \text{ s}^{-1}$. The concentration of HPO_4^{2-} decreases as $k_{\text{obsd}}/[\text{NH}_3]$ increases, so any contribution from $[\text{HPO}_4^{2-}]$ to the k_{obsd} value is much less than that of $[\text{H}_2\text{PO}_4^-]$.

Kinetics of HNCl_2 and NCl_3 Reaction. Dichloramine and trichloramine react with each other rapidly in neutral or basic solutions to give N_2 , Cl^- , and HOCl (eq 6). Dilute dichloramine solutions in the presence of 10% excess of ammonia are relatively stable at pH 6–7.⁹ The decomposition of trichloramine in solutions without ammonia present is also relatively slow in this pH range.¹³ Hence, it is possible to prepare solutions of each reactant in $\text{H}_2\text{PO}_4^-/\text{HPO}_4^{2-}$ buffer and keep them long enough to study their reaction by stopped-flow methods. Second-order unequal conditions (0.19–1.93 mM) are used and the reactions are monitored by the loss of NCl_3 at 360 nm. Substantial amounts of N_2 gas are observed when the concentrations are increased. The second-order rate constants (Table IV) increase as the $\text{p}[\text{H}^+]$ of the phosphate buffer increases from 6.13 to 6.88. Figure 7 shows that $k_{2\text{nd}}$ is directly proportional to the HPO_4^{2-} concentration. The rate expression for the reaction is given in eq 16, where the value for k_{HPO_4} is $2.92 (\pm 0.08) \times 10^4 \text{ M}^{-2} \text{ s}^{-1}$.



It is much more difficult to study the kinetics of the reaction between HNCl_2 and NCl_3 at high pH because the individual

(26) Nozaki, T.; Mise, T.; Torii, K. *Nippon Kagaku Kaishi* **1973**, 2030–2032.

(27) Hitch, B. F.; Mesmer, R. E. *J. Solution Chem.* **1976**, *5*, 667–680.

(28) Mesmer, R. E.; Baes, C. F. *J. Solution Chem.* **1974**, *3*, 307–321.

Table III. Pseudo-First-Order Rate Constants for the Reaction of Excess NH₃ with NCl₃^a

base or buffer (concn, M)	p[H ⁺]	[NH ₃] _T , M	k _{obsd} , s ⁻¹	
NaOH (0.050)		0.015	6.1 ± 0.1	
		0.020	7.2 ± 0.2	
		0.025	8.6 ± 0.1	
		0.030	9.4 ± 0.2	
		0.035	10.5 ± 0.5	
NaOH (0.075)		0.015	11.0 ± 0.3	
		0.020	12.4 ± 0.3	
		0.025	13.4 ± 0.3	
		0.030	15.5 ± 0.4	
		0.035	17.2 ± 0.3	
NaOH (0.100)		0.015	16.0 ± 0.5	
		0.020	18.0 ± 0.5	
		0.025	20.5 ± 0.5	
		0.030	23.0 ± 0.5	
		0.035	25.0 ± 0.5	
NaOH (0.125)		0.015	23.2 ± 0.4	
		0.020	26.5 ± 0.4	
		0.025	30 ± 1	
		0.030	31 ± 1	
		0.035	35 ± 1	
		10.13	0.100	0.477 ± 0.003
		9.93	0.100	0.39 ± 0.01
		9.88	0.100	0.376 ± 0.002
		9.74	0.100	0.30 ± 0.01
		9.73	0.100	0.313 ± 0.002
		9.51	0.100	0.229 ± 0.001
		9.51	0.100	0.227 ± 0.002
		9.42	0.100	0.209 ± 0.002
		9.34	0.100	0.176 ± 0.003
		9.32	0.100	0.165 ± 0.001
	9.25	0.100	0.148 ± 0.002	
	9.13	0.100	0.128 ± 0.001	
	8.92	0.100	0.086 ± 0.001	
	8.81	0.100	0.070 ± 0.001	
	10.03	0.080	0.225 ± 0.002	
	9.64	0.080	0.203 ± 0.001	
	9.48	0.080	0.173 ± 0.001	
	9.34	0.080	0.140 ± 0.001	
	9.15	0.080	0.098 ± 0.001	
	9.08	0.080	0.085 ± 0.002	
	8.99	0.080	0.073 ± 0.001	
	9.68	0.080	0.147 ± 0.001	
	9.44	0.080	0.113 ± 0.004	
	9.25	0.080	0.089 ± 0.001	
	9.04	0.080	0.067 ± 0.001	
	8.94	0.080	0.054 ± 0.002	
[PO ₄ ³⁻] _T (0.030)	11.06	0.010	0.71 ± 0.03	
	(0.040)	11.06	0.010	0.79 ± 0.01
	(0.050)	11.06	0.010	1.01 ± 0.04
	(0.060)	11.06	0.010	1.16 ± 0.04
	(0.070)	11.06	0.010	1.26 ± 0.03
[PO ₄ ³⁻] _T (0.050)	11.91	0.100	18.5 ± 0.2	
	11.81	0.100	22.9 ± 0.4	
	11.60	0.100	15.1 ± 0.1	
	11.49	0.100	15.7 ± 0.2	
	11.41	0.100	13.7 ± 0.2	
	11.40	0.100	12.4 ± 0.1	
	11.23	0.100	11.0 ± 0.3	
	11.13	0.100	10.0 ± 0.2	
	11.09	0.100	7.0 ± 0.3	
	11.01	0.100	6.0 ± 0.2	
	10.93	0.100	8.85 ± 0.3	
	10.54	0.100	3.0 ± 0.1	
	[PO ₄ ³⁻] _T (0.100)	6.85	0.100	6.55 (±0.01) × 10 ⁻³
		6.68	0.100	5.30 (±0.03) × 10 ⁻³
		6.55	0.100	4.3 (±0.1) × 10 ⁻³
6.38		0.100	3.6 (±0.1) × 10 ⁻³	
6.10		0.100	2.3 (±0.1) × 10 ⁻³	

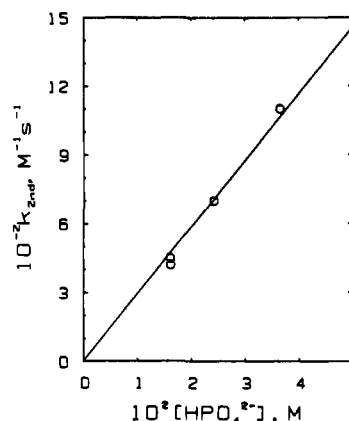
^aConditions: μ = 0.50 M, [NCl₃] = (3.5–4.1) × 10⁻⁴ M, 25.0 °C, λ_{obsd} = 360 nm.

reactants in the solutions decompose rapidly. We used the sequential-mixing mode of the Hi-Tech stopped-flow instrument to study the reactions in NaOH solutions. The NCl₃ solution

Table IV. Second-Order Rate Constants for the Reaction of HNCl₂ with NCl₃^a

10 ⁴ [HNCl ₂], M	10 ⁴ [NCl ₃], M	p[H ⁺]	k _{2nd} , M ⁻¹ s ⁻¹
2.68	2.33	6.13	4.5 (±0.7) × 10 ²
4.01	2.33	6.13	4.2 (±0.6) × 10 ²
4.12	2.00	6.42	7.0 (±0.5) × 10 ²
19.3	2.56	6.88	1.1 (±0.2) × 10 ³
4.96	1.89	12.42 ^b	> 2 × 10 ⁶

^aConditions: μ = 0.50 M, 25.0 °C, [PO₄³⁻]_T = 0.050 M, [NH₄⁺] ≈ [HNCl₂], λ_{obsd} = 360 nm. ^b[NaOH] = 0.050 M. pK_w = 13.72 (μ = 0.50 M, 25.0 °C).

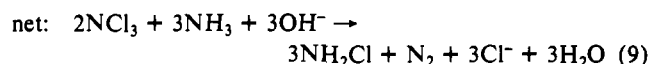
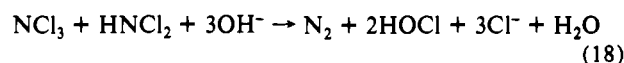
**Figure 7.** HPO₄²⁻ dependence of the k_{2nd} value for the reaction between HNCl₂ and NCl₃ at p[H⁺] 6.13–6.88.

(initially at pH 3.5) was mixed rapidly with an equal volume of 0.20 M NaOH just before it was mixed with HNCl₂ (initially at pH 4.0) and flowed into the Hi-Tech stopped-flow observation tube. The time for the premixing step is about 2 ms, which is much shorter than the half-life (72 ms) of the NCl₃ decomposition in 0.10 M NaOH,¹³ so relatively little loss occurs prior to mixing this solution with the HNCl₂ solution. The concentrations in the reactant mixture are 0.050 M OH⁻, 0.496 mM HNCl₂, 0.189 mM NCl₃, and ≈ 0.5 mM NH₃. The entire reaction is over within the 2.7-ms deadtime of the mixing cell,²² so the second-order rate constant for the reaction between HNCl₂ and NCl₃ must be greater than 2 × 10⁶ M⁻¹ s⁻¹ in 0.050 M OH⁻. The total absorbance change for the reaction is small and lower concentrations of reactants give too small of a signal to be detected easily. If the reaction has a [OH⁻] dependence similar to the [HPO₄²⁻] dependence found in eq 16, the value of the third-order rate constant for OH⁻ + HNCl₂ + NCl₃ must be greater than 4 × 10⁷ M⁻² s⁻¹.

Under all experimental conditions in this study, the reaction between NCl₃ and HNCl₂ is much faster than the reaction between NCl₃ and excess NH₃. Therefore, two NCl₃ molecules are consumed each time one NCl₃ reacts with NH₃ in accord with the rate expression in eq 7.

Discussion

The first step in the reaction between NCl₃ and NH₃ is a base-assisted (or acid-assisted) transfer of Cl⁺ to give HNCl₂ and NH₂Cl (eq 17). This is followed by a rapid reaction between



HNCl₂ and NCl₃ to give N₂, Cl⁻, and HOCl (eq 18). The HOCl produced reacts with excess NH₃ to form more NH₂Cl (eq 19) and the overall reaction is the sum of eqs 17–19 as given in eq 9. This accounts for the observed stoichiometry which three

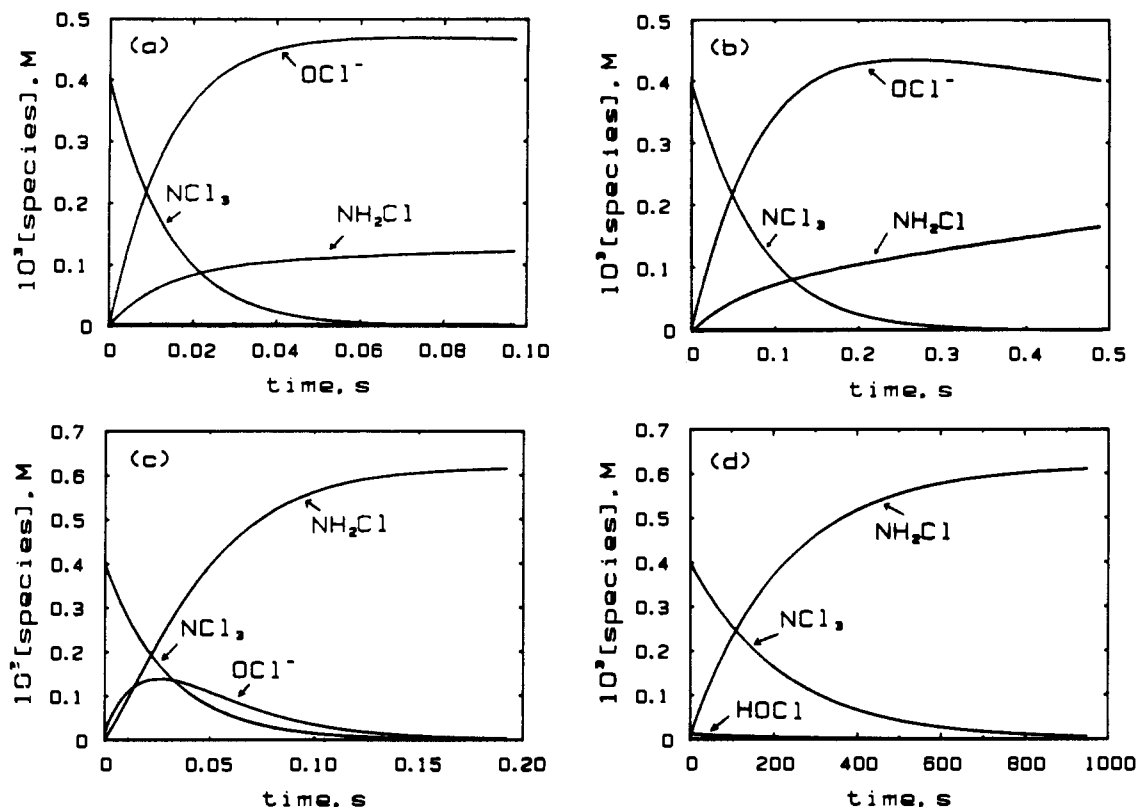


Figure 8. Plots of concentration of chlorine species vs time by GEAR calculation ($[\text{NCl}_3]_i = 4 \times 10^{-4} \text{ M}$, $[\text{OCl}^-]_T = 2 \times 10^{-5} \text{ M}$): (a) $[\text{OH}^-] = 0.125 \text{ M}$, $[\text{NH}_3]_T = 0.035 \text{ M}$; (b) $[\text{OH}^-] = 0.050 \text{ M}$, $[\text{NH}_3]_T = 0.015 \text{ M}$; (c) pH 11.34, $[\text{PO}_4^{3-}]_T = 0.05 \text{ M}$, $[\text{NH}_3]_T = 0.1 \text{ M}$; (d) pH 6.10, $[\text{PO}_4^{3-}]_T = 0.1 \text{ M}$, $[\text{NH}_3]_T = 0.1 \text{ M}$.

NH_2Cl molecules are formed from two NCl_3 molecules (Table II). We can rule out direct N-N bond formation between NH_3 and NCl_3 (eq 20). Such a reaction would release no HOCl and



would form no NH_2Cl . Hence a chlorine-transfer step (eq 17) is needed to initiate the reaction. The observed stoichiometry also eliminates direct N_2 formation by the reaction between NHCl_2 and NH_2Cl .

We know from other studies that NH_2Cl also reacts with NCl_3 ²⁹ and with HOCl ⁶ to give more HNCl_2 (Table V); however, these reaction rates are too slow to compete with the NH_3 and NCl_3 reaction under our experimental conditions. The reaction in eq 17 is a general-base-assisted reaction in accord with the rate expression in eq 21, where the value of k_B ($\text{M}^{-2} \text{s}^{-1}$) is 4.46×10^3

$$-d[\text{NCl}_3]/dt = 2k_B[\text{B}][\text{NH}_3][\text{NCl}_3] \quad (21)$$

for OH^- , 3.3×10^3 for PO_4^{3-} , and 22 for NH_3 . When B is H_2O , the second-order rate constant is $2.2 \text{ M}^{-1} \text{s}^{-1}$ as evaluated from the data in the ammonia-buffered study. (The precision of the $k_{\text{H}_2\text{O}}$ value as measured from the NH_3 buffer data is much better than the precision of the $k_{\text{H}_2\text{O}}$ value as measured from the $\text{HPO}_4^{2-}/\text{PO}_4^{3-}$ data, because of the scatter of data in Figure 5. We also believe that the value of $2.2 \pm 0.1 \text{ M}^{-1} \text{s}^{-1}$ is more reliable than the $k_{\text{H}_2\text{O}}$ value estimated from the $\text{H}_2\text{PO}_4^-/\text{HPO}_4^{2-}$ data in Figure 6, where small contributions of general-base assistance from HPO_4^{2-} or even small contributions from acid assistance by H^+ cannot be ruled out.)

The reaction in eq 17 is also a general-acid-assisted one (eq 22), where the value of k_{HB} is $450 \text{ M}^{-2} \text{s}^{-1}$ for H_2PO_4^- . Of course, the ammonia concentration is reduced as the acidity of the solution is increased and this causes an overall decrease in the rate of the reaction in eq 22.

$$-d[\text{NCl}_3]/dt = 2k_{\text{HB}}[\text{HB}][\text{NH}_3][\text{NCl}_3] \quad (22)$$

Table V. Summary of the Reactions and Rate Constants Used in the GEAR Program^a

reactions	rate const
$\text{NH}_3 + \text{NCl}_3 + \text{OH}^-$ (eq 17)	$4.46 (\pm 0.06) \times 10^3 \text{ M}^{-2} \text{s}^{-1}$
$\text{NH}_3 + \text{NCl}_3 + \text{PO}_4^{3-}$ (eq 17)	$3.3 (\pm 0.4) \times 10^3 \text{ M}^{-2} \text{s}^{-1}$
$\text{NH}_3 + \text{NCl}_3 + \text{NH}_3$ (eq 17)	$22 (\pm 1) \text{ M}^{-2} \text{s}^{-1}$
$\text{NH}_3 + \text{NCl}_3$ (eq 17)	$2.2 (\pm 0.1) \text{ M}^{-1} \text{s}^{-1}$
$\text{NH}_3 + \text{NCl}_3 + \text{H}_2\text{PO}_4^-$ (eq 17)	$450 (\pm 20) \text{ M}^{-2} \text{s}^{-1}$
$\text{NH}_2\text{Cl} + \text{NCl}_3 + \text{OH}^-$	$1.57 \times 10^5 \text{ M}^{-2} \text{s}^{-1b}$
$\text{NH}_2\text{Cl} + \text{NCl}_3 + \text{PO}_4^{3-}$	$1.1 \times 10^4 \text{ M}^{-2} \text{s}^{-1b}$
$\text{HNCl}_2 + \text{NCl}_3 + \text{OH}^-$ (Scheme II)	$10^8 \text{ M}^{-2} \text{s}^{-1}$
$\text{HNCl}_2 + \text{NCl}_3 + \text{HPO}_4^{2-}$ (Scheme II)	$2.92 (\pm 0.06) \times 10^4 \text{ M}^{-2} \text{s}^{-1}$
$\text{NCl}_3 + \text{OH}^-$	$8 (\pm 3) \text{ M}^{-1} \text{s}^{-1c}$
$\text{NCl}_3 + 2\text{OH}^-$	$890 (\pm 30) \text{ M}^{-2} \text{s}^{-1c}$
$\text{HOCl} + \text{NH}_3$	$2.8 \times 10^6 \text{ M}^{-1} \text{s}^{-1d}$
$\text{HOCl} + \text{NH}_2\text{Cl}$	$150 \text{ M}^{-1} \text{s}^{-1d}$

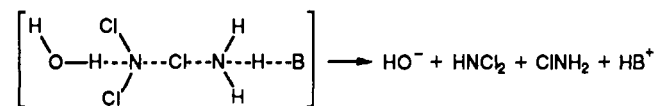
^a Conditions: $\mu = 0.50 \text{ M}$, $25.0 \text{ }^\circ\text{C}$. This work except where noted. $\text{p}K_a = 7.44$ for HOCl , $\mu = 0.10 \text{ M}$, $25.0 \text{ }^\circ\text{C}$ in ref 6. $\text{p}K_a = 6.46$ for H_2PO_4^- , $\mu = 0.50 \text{ M}$, $25.0 \text{ }^\circ\text{C}$ in ref 28. $\text{p}K_a = 9.32$ for NH_4^+ , $\mu = 0.50 \text{ M}$, $25.0 \text{ }^\circ\text{C}$ in ref 26. $\text{p}K_a = 11.34$ for HPO_4^{2-} , $\mu = 0.50 \text{ M}$, $25.0 \text{ }^\circ\text{C}$ in ref 27. ^b Reference 29. ^c Reference 13. ^d Reference 6.

GEAR Simulations. GEAR^{30,31} is a computer program that can be used to calculate concentrations as a function of time for multiple reactions. There are many competitive reactions to be considered in the NCl_3 and NH_3 mixture. Figure 8a–d shows the calculated concentrations of the chlorine species versus time for four sets of conditions. The calculations are based on the rate constants and the $\text{p}K_a$ values given in Table V. In Figure 8a, the high concentration of OH^- (0.125 M) causes the OCl^- concentration to build up in the 0.1-s time window shown. This buildup is a result of (1) direct attack of OH^- on NCl_3 ,¹³ (2) the reaction of the HOCl produced in eq 18 with OH^- , and (3) the slower

(30) Beukelman, T. E.; Chesick, K.; McKinney, R. J.; Weigert, F. J. GEAR. E. I. du Pont de Nemours and Co., Wilmington, DE.

(31) GEAR is a modification of the HAVCHM program: Stabler, R. N.; Chesick, J. *Int. J. Chem. Kinet.* **1978**, *10*, 461–469.

Scheme I. Base-Assisted Reaction Path



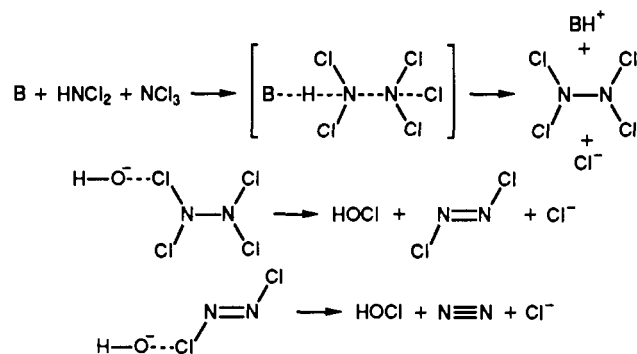
formation of NH_2Cl from the reaction in eq 19 when the $[\text{OCl}^-]/[\text{HOCl}]$ ratio is large.⁶ Over a longer period of time, the OCl^- concentration decreases and more NH_2Cl forms. This is seen in Figure 8b with a time window of 0.5 s for the reactions in 0.05 M OH^- . At $\text{p}[\text{H}^+]$ 11.34, Figure 8c shows that the maximum OCl^- concentration forms at 0.025 s and that it is completely converted to NH_2Cl within 0.2 s. The decay of NCl_3 is relatively rapid as shown in Figure 8c because both phosphate and ammonia are present in high concentrations. Figure 8d shows the behavior at $\text{p}[\text{H}^+]$ 6.1 where the NCl_3 decay is slower and there is very little buildup of HOCl . Negligible concentrations of HNCl_2 are present for all four sets of conditions because of the rapid reaction between NCl_3 and HNCl_2 . The calculated GEAR curves for the loss of NCl_3 are analyzed as first-order reactions. The results give rate constants that agree with the experimental k_{obsd} values. These calculations are based on the assumption that the third-order rate constant for $\text{OH}^- + \text{HNCl}_2 + \text{NCl}_3$ is $10^8 \text{ M}^{-2} \text{ s}^{-1}$. All the other rate constants in Table V are experimental values. The GEAR simulations are significant because they are consistent with the observed first-order decay of NCl_3 , with the mechanism proposed in eqs 17–19, and with the overall stoichiometry (after 20 min).

Mechanisms of Cl^+ Transfer. Scheme I shows the proposed transition state for the base-assisted reaction of NCl_3 with NH_3 to form HNCl_2 and NH_2Cl . In the base-assisted reactions Cl^+ -transfer is assisted by H^+ removal from NH_3 . This cannot be a preequilibrium step to give NH_2^- , because the reactions are general-base-assisted ones (i.e. by NH_3 , PO_4^{3-} , and OH^-) and preequilibration would give only specific-base catalysis (i.e. acceleration only by OH^-). We propose that a water molecule assists in the formation of HNCl_2 as Cl^+ transfer occurs.

The proposed acid-assisted mechanism and transition state is very similar to the base-assisted case except that H_2PO_4^- rather than H_2O donates a proton to form HNCl_2 and H_2O rather than B now acts as the proton acceptor as ClNH_3^+ forms.

Other examples of acid-assisted Cl^+ transfer are seen in the reaction of SO_3^{2-} with NH_2Cl ²⁵ as well as the reactions of I^- with OCl^- , NH_2Cl , HNCl_2 ,¹⁶ and HOCl .³² Base-assisted Cl^+ transfer

Scheme II



is seen in the reactions of HOCl with HNCl_2 .⁹ Specific-base/general-acid-assisted Cl^+ transfer is seen in the base decomposition of NCl_3 in aqueous solution.¹³

Mechanism of N_2 Formation. Scheme II shows the proposed transition state for the base-assisted reaction of HNCl_2 and NCl_3 . The base B (OH^- , PO_4^{3-} , or NH_3) helps to remove the proton from HNCl_2 as it reacts with NCl_3 to displace Cl^- . We propose that the first product is tetrachlorohydrazine (N_2Cl_4), which decomposes rapidly by OH^- attack to remove Cl^+ and the formation of a $\text{N}=\text{N}$ double bond with Cl^- elimination to give $\text{Cl}-\text{N}=\text{N}-\text{Cl}$. This reacts by a similar mechanism to give another HOCl molecule, N_2 , and Cl^- . The initial base-assisted reaction between HNCl_2 and NCl_3 is much more favorable than the corresponding reactions of $\text{OH}^- + \text{NCl}_3 + \text{NCl}_3$ or $\text{OH}^- + \text{HNCl}_2 + \text{HNCl}_2$. This indicates that OH^- and HNCl_2 are needed to generate a strong nucleophile (NCl_2^-) that can react with a strong electrophile (NCl_3) to form a $\text{N}-\text{N}$ bond and to eliminate Cl^- . The $\text{N}-\text{Cl}$ bond strength of NCl_3 is weaker than that of HNCl_2 , so it is easier to eliminate Cl^- from NCl_3 . The speed of the base-assisted reaction between HNCl_2 and NCl_3 is remarkable. In 0.1 M OH^- , the rate constant for the $\text{HNCl}_2 + \text{NCl}_3$ reaction is more than 10^{10} times greater than the rate constant for hydrazine formation from $\text{NH}_3 + \text{NH}_2\text{Cl}$.⁸ There appears to be no information about the proposed N_2Cl_4 and N_2Cl_2 intermediates, but the driving force to form N_2 should be very favorable and they would be expected to be short-lived intermediates in base.

Acknowledgment. This work was supported by National Science Foundation Grant CHE-8720318.

(32) Nagy, J. C.; Kumar, K.; Margerum, D. W. *Inorg. Chem.* **1988**, *27*, 2773–2780.